CHEMISTRY OF MATERIALS

Article

pubs.acs.org/cm

Molten-Salt-Mediated Syntheses of Sr_2FeReO_6, Ba_2FeReO_6, and Sr_2CrReO_6: Particle Sizes, B/B′ Site Disorder, and Magnetic Properties

Lindsay Fuoco, Dianny Rodriguez, Tim Peppel, and Paul A. Maggard*

Department of Chemistry, North Carolina State University, Raleigh, North Carolina 27695-8204, United States

Supporting Information

ABSTRACT: The half-metallic double-perovskites Sr_2FeReO_6, Ba_2FeReO_6, and Sr_2CrReO_6 were synthesized in high purity and homogeneity using a NaCl/KCl molten flux at 750−800 °C in as little as 3−6 h. The particle sizes could be varied from ∼50 nm to >1 μm depending on the specific flux conditions and the double-perovskite composition. Powder X-ray diffraction refinements were used to characterize the extent of B/B′ site disorder (i.e., Fe/Re or Cr/Re sites), and that ranged from ∼83−85% for Sr_2FeReO_6, ∼90−97% for Ba_2FeReO_6, and ∼84−90% for Sr_2CrReO_6. The magnetic properties were measured as a function of magnetic field strength and analyzed with respect to the extent of B/B′ site ordering and resultant particle sizes that ranged from ∼50−500 nm for Sr_2FeReO_6, ∼100−800 nm for Sr_2CrReO_6, and ∼250 nm to 2 μm for Ba_2FeReO_6. Further, large temperature-dependent magnetoresistivites were observed for the flux-prepared Sr_2FeReO_6, Ba_2FeReO_6, and Sr_2CrReO_6, which are attributed to high concentrations of grain boundaries present.

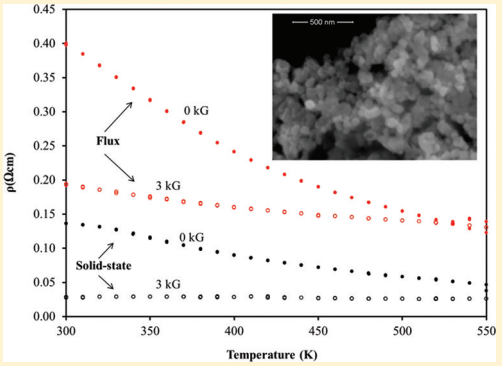

KEYWORDS: *double perovskites, flux-mediated synthesis, magnetoresistance*

INTRODUCTION

The double-perovskites of the composition $A_2BB'O_6$ (A = Sr or Ba; B = Fe or Cr; B′ = Mo or Re) have been the focus of intense research interest owing to the discovery of high magnetic-ordering transition temperatures and the half-metallic properties of Sr_2FeMoO_6 (T_c ∼ 415K), Sr_2FeReO_6 (T_c ∼ 400K), Sr_2CrReO_6 (T_c ∼ 635 K), and others.[1−5] Interestingly, large magnetoresistances have been measured in their polycrystalline forms that result from spin-polarized intergrain tunneling across the grain boundaries, and as expected, is absent in the analogous single-crystal measurements.[6] A spin-dependent transport mechanism was first proposed and found in metal oxides such as for $La_{2/3}Sr_{1/3}MnO_3$.[7] In these $A_2BB'O_6$ double-perovskites, the magnetic properties exhibit a strong dependence on the resulting grain sizes and the extent of B/B′ site disorder present in their structures, and which in turn depend closely on the synthesis conditions.[8−10] In Sr_2FeMoO_6, for example, the formation of much smaller particles has been shown to yield significant enhancements in the intergrain tunneling-magnetoresistance (i.e., ITMR) of multigrain samples.[10−12] However, high-purity and homogeneity are typically difficult to obtain for reduced rhenates (i.e., Re^{5+}/Re^{6+}) owing to their refractive nature. Members of the reduced rhenate family must predominantly be prepared according to relatively demanding solid-state procedures that involve multiple heating cycles (>1−2 weeks), carefully controlled reducing conditions inside sealed fused-silica ampules, and temperatures up to 1200 °C. Thus, more rapid and efficient routes that target high-purity, homogeneous, and tunable distributions of particle sizes are needed for probing their magnetic properties in polycrystalline forms.

The use of molten-salt fluxes can potentially yield a significantly greater flexibility to modulate metal-oxide particle sizes and microstructures via selection of the amount and type of flux, reaction time and temperature, and also cooling rates.[13−16] Flux-mediated syntheses can allow for metal-oxide particles to form at relatively fast rates (<1 h) and in a more well-faceted and homogeneous distribution of sizes that arise from the enhanced mobility of the metal-oxide reactants. For example, molten-salt mixtures of Na_2SO_4/K_2SO_4 and NaCl/KCl have been used to prepare the layered perovskites $Bi_5Ti_3FeO_{15}$ and $La_2Ti_2O_7$ in high purity in only 0.5 h with platelet morphologies and tunable particle sizes of down to <100 nm in thickness and ∼500−5000 nm on the edges.[13,15] However, to the best of our knowledge, the flux synthetic method has never previously been reported for the preparation of reduced-rhenate compositions (i.e., containing Re^{5+} or Re^{6+}). Reported herein are the flux-mediated syntheses of three reduced-rhenate members of the $A_2BB'O_6$ double-perovskite family, Sr_2FeReO_6, Ba_2FeReO_6, and Sr_2CrReO_6, using a eutectic NaCl/KCl salt mixture. The flux amounts, heating durations and cooling rates were controlled and investigated for their effect on particle sizes, extent of B/B′ site ordering, as well as magnetic and electrical properties.

Received: August 25, 2011
Revised: November 10, 2011
Published: November 14, 2011

dx.doi.org/10.1021/cm202545z | *Chem. Mater.* 2011, 23, 5409−5414

Table 1. Powder X-ray Diffraction Refinement Results for Sr_2FeReO_6 (Space Group $I4/m$)

Sr_2FeReO_6[a]	0.5:1, 3 h	0.5:1, 12 h	1:1, 3 h	1:1, 12 h	solid state
		Lattice Constants			
a (Å)	5.5672(3)	5.5644(4)	5.5649(4)	5.5655(2)	5.5585(3)
c (Å)	7.9003(8)	7.8962(8)	7.8986(9)	7.8990(7)	7.8969(5)
		Fractional B and B′ Site Occupancies			
Fe1 (0,0,0)	0.8354(3)	0.8440(3)	0.8391(2)	0.8476(2)	0.9702(2)
Re1 (0,0,0)	0.1654	0.1559	0.1609	0.1523	0.0297
Re2 (0,0,0.5)	0.8354	0.8440	0.8391	0.8476	0.9702
Fe2 (0,0,0.5)	0.1654	0.1559	0.1609	0.1523	0.0297

[a]Synthesis conditions given as the flux-to-product molar ratio (#:#), reaction time (#h), and cooling time (#h) if other than radiatively cooled.

Table 2. Powder X-ray Diffraction Refinement Results for Ba_2FeReO_6 (Space Group $Fm\bar{3}m$)

Ba_2FeReO_6[a]	1:1, 6 h	3:1, 6 h	3:1, 6 h, quench	3:1,6 h, 24 h
		Lattice Constant		
a (Å)	8.0540(3)	8.0533(3)	8.0536(4)	8.0548(7)
		Fractional B and B′ Site Occupancies		
Fe1 (0,0,0)	0.90627(6)	0.94088(4)	0.90504(5)	0.96947(5)
Re1 (0,0,0)	0.09373	0.05912	0.09496	0.03053
Re2 (0.5,0.5,0.5)	0.90627	0.94088	0.90504	0.96947
Fe2 (0.5,0.5,0.5)	0.09373	0.05912	0.09496	0.03053

[a]Synthesis conditions given as the flux-to-product molar ratio (#:#), reaction time (#h), and cooling time (#h) if other than radiatively cooled.

EXPERIMENTAL SECTION

Synthesis. Flux syntheses of Sr_2FeReO_6, Ba_2FeReO_6, and Sr_2CrReO_6 were performed by first combining mixtures of analytical reagent grade SrO (Alfa Aeasar, 99.5%), BaO (Alfa Aeasar, 99.5%), Cr_2O_3 (Sigma Aldrich, 99%), Fe_3O_4 (Alfa Aeasar, 99%), Re_2O_7 (Alfa Aesar, 99.995%), and Re (Alfa Aesar, 99.99%) inside a glovebox under a nitrogen atmosphere (total weight = 0.6 g). The loaded Re:Re_2O_7 molar ratio for Sr_2FeReO_6 was stoichiometric (5:8 ratio), while reactions for Ba_2FeReO_6 and Sr_2CrReO_6 needed to be loaded more Re_2O_7-rich (4.6:8 and 2:6 ratios, respectively) in order to achieve highly pure phases. The reactants were ground together and combined with a eutectic NaCl/KCl (Fisher, 99%; dehydrated) mixture to give flux:product molar ratios of 0.5:1 and 1:1 for Sr_2FeReO_6, and 1:1 and 3:1 for Ba_2FeReO_6 and Sr_2FeReO_6. These reactant mixtures were flame-sealed inside evacuated fused-silica ampules (length = 90 mm, i.d. = 8 mm) and heated to 750 °C for Sr_2FeReO_6 for 3−12 h, or to 800 °C for both Sr_2CrReO_6 and Ba_2FeReO_6 for 6 h. The reactions were then either quenched, slow cooled to 550 °C at rates of 5 or 10 °C per hour, or radiatively cooled to room temperature. The resulting products were washed with hot deionized water to remove the NaCl/KCl flux. Further increases in the flux amounts were unsuccessful and resulted in impurities. For comparison, the standard solid-state synthesis of Sr_2FeReO_6 was performed by using a slightly modified procedure from the literature,[17] which involved the preparation of a $Sr_4Re_2O_{11}$ precursor by combining stoichiometric amounts of $SrCO_3$ and Re_2O_7 and heating in alumina crucibles in air at 1100 °C for 6 h. The $Sr_4Re_2O_{11}$ precursor compound was then combined with Fe_2O_3 and Fe and ground together with a mortar and pestle in a glovebox under a nitrogen atmosphere (total weight = 0.6 g). The resulting mixture was flame-sealed inside an evacuated silica ampule and heated at 910 °C for 72 h followed by intermittent grinding and heating to 960 °C for 72 h. Powder X-ray diffraction analysis revealed a small Re impurity phase (∼5%) still present in the solid-state reaction product.

Characterization. High-resolution powder X-ray diffraction data sets were collected for all samples at room temperature on a Rigaku R-Axis Spider with a curved image plate detector and Cu Kα_1 radiation from a sealed-tube X-ray source. Refinements were performed by the Rietveld method using the WPF refinement option in Jade 9.[18] In a typical refinement, initially only the zero-point shift and scale factor were refined. The lattice constants and background parameters were then allowed to refine followed by the oxygen positions. This was followed by refinement of the isotropic thermal parameters, and which thereafter were fixed to refine the Fe/Re or Cr/Re site occupancies. The thermal parameters were then released in the last stage of the refinement. Two metals disordered over the same site were assigned to have the same thermal displacement parameters. The thermal displacement parameters for the oxygen atomic positions were also set to be equal. Powder refinement parameters are given in Tables 1, 2 and 3 for Sr_2FeReO_6, Ba_2FeReO_6, and Sr_2CrReO_6, respectively, and resulting fits of the Rietveld refinements to the experimental powder data are plotted in Figure 1. More complete tables of all refinement parameters are provided in the Supporting Information.

Table 3. Powder X-ray Diffraction Refinement Results for Sr_2CrReO_6 (Space Group $Fm\bar{3}m$)

Sr_2CrReO_6[a]	1:1, 6 h	3:1, 6 h	3:1,6 h, quench	1:1,6 h, 48 h
		Lattice Constant		
a (Å)	7.8077(5)	7.8080(3)	7.8075(5)	7.8085(5)
		Fractional B and B′ Site Occupancies		
Fe1 (0,0,0)	0.87343(5)	0.84815(3)	0.83813(4)	0.9007(3)
Re1 (0,0,0)	0.12657	0.15186	0.16187	0.0993
Re2 (0.5,0.5,0.5)	0.87343	0.84815	0.83813	0.9007
Fe2 (0.5,0.5,0.5)	0.12657	0.15186	0.16187	0.0993

[a]Synthesis conditions given as the flux-to-product molar ratio (#:#), reaction time (#h), and cooling time (#h) if other than radiatively cooled.

Scanning electron microscopy (SEM) was performed on an FEI Quanta 200 and used to investigate the particle microstructures and sizes as a function of flux-preparation conditions. Field-dependent magnetization measurements were taken on ∼50 mg of the powdered samples from −7 to 7 T at 5K using a Quantum Design MPMS XL SQUID. Electrical resistivity measurements were performed on high-purity pelletized samples without annealing using the four probe method (Hall effect instrument; MMR Technologies) at magnetic field strengths extending from 0 to 3 kG over a temperature range of 300−550 K.

dx.doi.org/10.1021/cm202545z | Chem. Mater. 2011, 23, 5409−5414

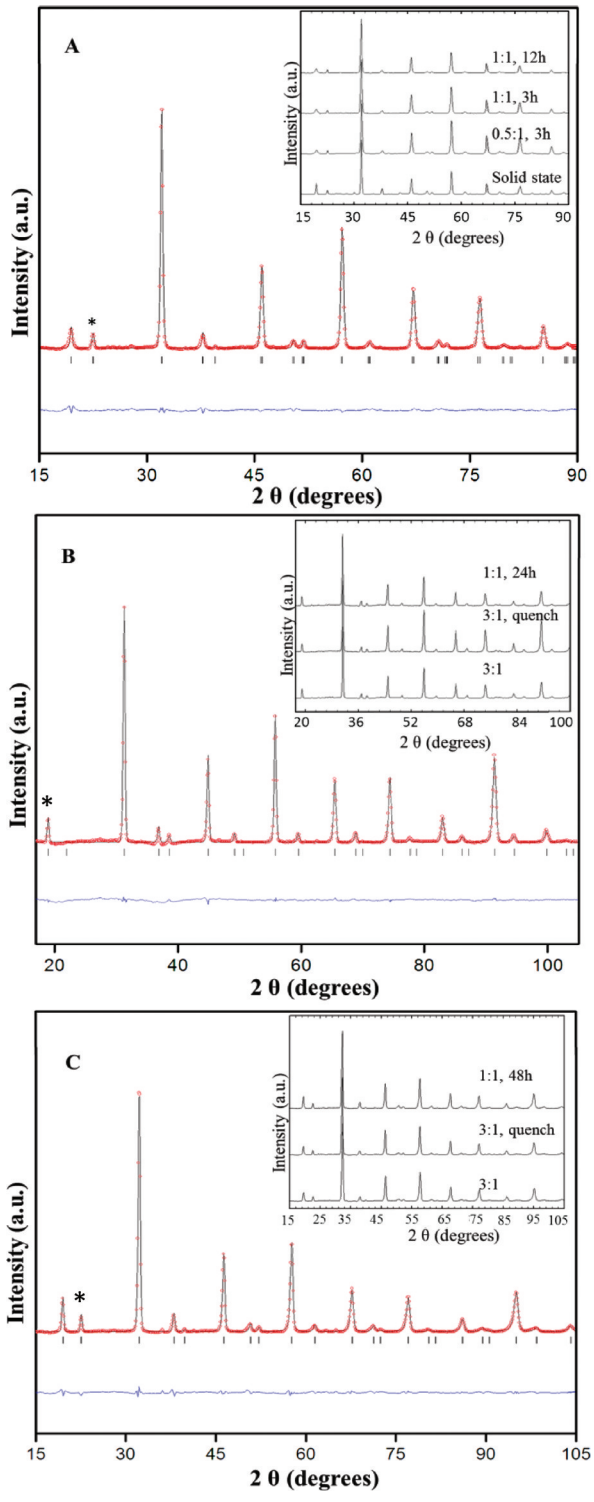

Figure 1. PXRD Rietveld refinement results for (A) Sr_2FeReO_6 synthesized using a 0.5:1 flux for 12 h; (B) Ba_2FeReO_6 at a 1:1 flux and radiatively cooled; and (C) Sr_2CrReO_6 at a 1:1 flux ratio. Observed profiles are indicated by the circles and the calculated profiles by the solid lines. Bragg peak positions are indicated by vertical peaks, and the difference diffractogram is shown at the bottom. The main (111) or (101) superstructure reflections are labeled with an asterisk for each phase.

RESULTS AND DISCUSSION

Structure Refinements and Particle Characterization. The double-perovskite structure of Sr_2FeReO_6 exhibits a rock-salt type ordering of the Fe/Re transition metals in a parent ABO_3 perovskite-type structure that also exhibits a small tetragonal distortion (space group: $I4/m$).[4] The related structures of Sr_2CrReO_6 and Ba_2FeReO_6 also exhibit a rock-salt ordering of the Cr/Re and Fe/Re cations and crystallize in the non-distorted cubic crystal system (space group: $Fm\bar{3}m$).[4,19] The powder X-ray diffraction (PXRD) patterns for the flux and solid-state-prepared Sr_2FeReO_6, Ba_2FeReO_6, and Sr_2CrReO_6 products are shown in Figure 1. These confirm that each could be synthesized using a molten NaCl/KCl flux in high purity in reaction times of only ~3−6 h. Rietveld refinements of the PXRD data for all samples were carried out and the resultant lattice parameters, atomic coordinates, and B/B′ site occupancies are provided in Tables 1, 2, and 3. Rietveld refinement profiles for each are shown in Figure 1. Rietveld refinement profiles for all other samples are provided in the Supporting Information. The extent of B/B′ (e.g., Fe/Re) ordering is reflected in the peak intensities of the main superstructure (111) reflections for Ba_2FeReO_6 and Sr_2CrReO_6, or the analogous (101) superstructure reflection for Sr_2FeReO_6. These characteristic peaks are present in all the flux-synthesized and solid-state Sr_2FeReO_6, Ba_2FeReO_6, and Sr_2CrReO_6 products and their positions have been indicated in Figure 1.

Powder X-ray refinement results listed in Table 1 show that the degree of B/B′ site ordering obtained for the flux-prepared Sr_2FeReO_6 samples was ~83−85% with relatively little variation except for a slightly higher ordering found for the 12 h versus 3 h reaction times. Conversely, the Sr_2FeReO_6 sample, prepared by solid-state methods over the course of one week of heating, was found to show an ~97% complete Fe/Re site ordering, consistent with previously reported preparations.[2,20] For Ba_2FeReO_6, the degree of Fe/Re site ordering ranged from ~90−97%, with the highest ordering found for the longest reaction time of 24 h. This is somewhat lower than the ~97% Fe/Re ordering obtained by solid-state methods at much longer reaction times.[19] The Cr/Re ordering for the flux-prepared Sr_2CrReO_6 products ranged from ~84−90%, with the highest ordering of ~90% for the 1:1 flux reaction that was slow cooled over 2 days and the lowest ordering of ~84% for the 3:1 flux reaction that was quenched after 6 h. Previously reported solid-state preparations of Sr_2CrReO_6 resulted in an ~77−87% Cr/Re ordering, a little lower but comparable to our flux preparations.[4,21,22] Thus, although there is a significant trade-off in the extent of B/B′ site ordering for shorter flux-reaction times in Sr_2FeReO_6, there is little to almost no significant effect of the shorter flux-reaction times for Ba_2FeReO_6 and Sr_2CrReO_6.

Representative scanning electron microscopy (SEM) images of the flux products for Sr_2FeReO_6, Ba_2FeReO_6, and Sr_2CrReO_6 are given in Figures 2 and 3 for both the smallest and largest particle-size distributions typically found for each. All SEM images revealed homogeneous distributions of aggregated block-like particles that, depending on the particular double-perovskite and the flux reaction conditions, could be varied in size from ~50 nm to >1 μm. The smallest particle sizes of ~50 nm could be prepared for Sr_2FeReO_6 using a 1:1 or 0.5:1 flux:product molar ratio reacted for only 3 h, shown in Figure 2 (A and C). These particles could be increased in size up to ~500 nm by increasing the reaction time to 12 h, Figure 2B. By contrast, the variation of flux reaction conditions (i.e., flux amount, reaction time) had a relatively much smaller effect on the particle sizes and distributions for either Ba_2FeReO_6 or Sr_2CrReO_6. For Ba_2FeReO_6, shown in Figure 2 (A, B, and C), relatively larger particles of >1 μm were formed after only a 6 h reaction time using either 1:1 or 3:1 flux ratios. Quenching this reaction

dx.doi.org/10.1021/cm202545z | Chem. Mater. 2011, 23, 5409−5414

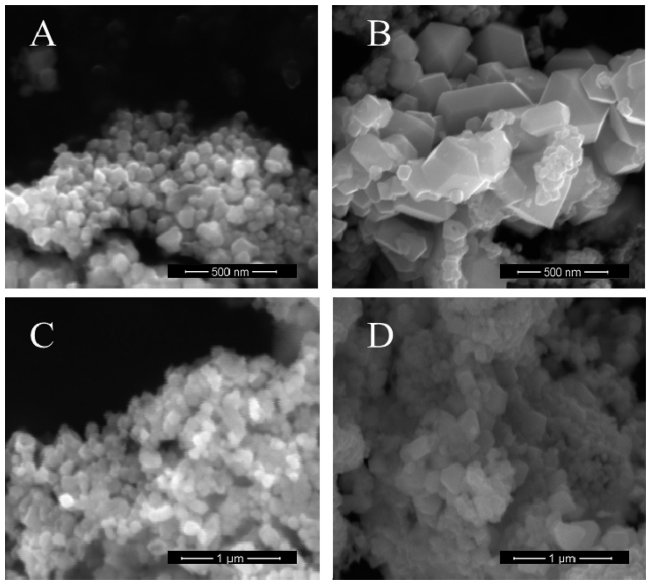

Figure 2. SEM images for Sr_2FeReO_6 synthesized using a molten NaCl/KCl flux at (A) 0.5:1 ratio for 3 h, (B) 0.5:1 ratio for 12 h, (C) 1:1 ratio for 3 h, and (D) 1:1 ratio for 12 h.

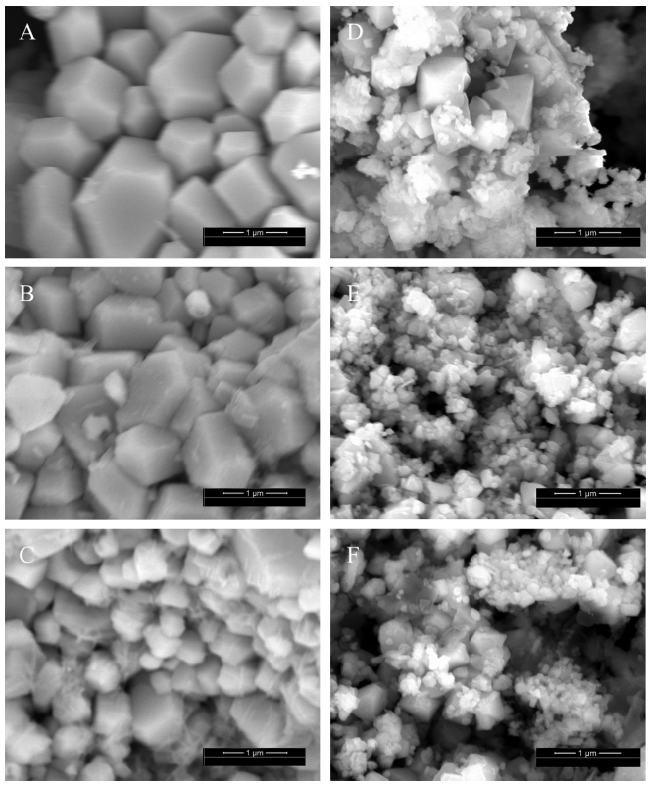

Figure 3. SEM images for Ba_2FeReO_6 synthesized using a molten NaCl/KCl flux at (A) a 1:1 ratio for 6 h, (B) 3:1 ratio for 6 h, (C) a 3:1 ratio for 6 h and quenching; Sr_2CrReO_6 using (D) a 1:1 ratio for 6 h, (E) a 1:1 ratio and slow cooling over 24 h, and (F) a 3:1 ratio for 6 h and quenching. Samples in A, B, and D were radiatively cooled.

produced only slightly smaller particles, Figure 3C. While for Sr_2CrReO_6, shown in Figure 2 (D, E, and F), a mixture of both smaller ~50−100 nm particles and larger ~500 nm particles nearly always resulted. Either quenching or slow cooling these reactions only resulted in small changes in the distribution of smaller versus larger particles. While, in general, the particle sizes decreased with increasing amounts of flux and with faster cooling rates, the rate of particle growth in the NaCl/KCl flux was significantly more variable for Sr_2FeReO_6 than for either Ba_2FeReO_6 or Sr_2CrReO_6. For the latter two compounds, the relatively small changes in particle sizes with faster cooling rates, as well as low amount of flux necessary for their synthesis, seem to indicate these reactions likely proceed by a flux-assisted mechanism.

Magnetic Properties. Each of the Sr_2FeReO_6, Ba_2FeReO_6, and Sr_2CrReO_6 double-perovskites exhibits a high-temperature magnetic ordering that stems from the ferromagnetic arrangement of localized spins on Fe^{3+}/Cr^{3+} ($S = 5/2$ and 3/2, respectively) that are ferromagnetically coupled via the delocalized and antiparallel Re^{5+} ($S = 1$) spins. Their Curie temperatures are all higher than room temperature, at T_c = ~400, ~303, and ~635 K, respectively. Thus, in order to determine the effect of the flux reaction conditions on their magnetic properties, measurements of their magnetization versus applied field was measured, shown in Figure 4. Summarized in Table 4 are the spontaneous and remanent magnetizations (M_s and M_r respectively), the coercive field (H_c), and the % ordering of the B/B′ cation sites as obtained from the powder X-ray refinements. However, at the maximum applied field of 7 T, magnetization saturation cannot be completely reached for any of the compounds. Previous reports have shown that their maximum saturation magnetization can typically only be achieved by high magnetic fields approaching ~30 T.[22,23] The magnetization at 7 T for all of the flux-prepared Sr_2FeReO_6 products ranged from ~1.57−2.17 μB and were lower than the expected 3.0 μ_B from the antiparallel alignment of the Fe^{3+}/Re^{5+} spins. Lower values for the saturation magnetization have also been previously correlated with the extent of B/B′ site disorder.[8,24] However, in these cases, the % B/B′ site disorder is relatively constant at ~83−85%. In the case of Sr_2FeMoO_6, decreased particle sizes have also been found to increase the amount of magnetically disordered grain boundaries and thus found to also contribute to a decreased saturation magnetization.[3,10,25,26] The flux synthesis of Sr_2FeReO_6 showed the largest range of attainable particle sizes, but any relationships to the magnetic data remain unclear. For the Ba_2FeReO_6 flux-prepared products, a smaller H_c and larger M_s values of from ~2.10−2.40 μ_B were observed. In this case, the higher Fe/Re site ordering of the cations results in significantly higher M_s and M_r values, but a lower H_c as compared to Sr_2FeReO_6. Furthermore, the larger particle sizes of Ba_2FeReO_6 also serve to decrease the amount of grain boundaries that are magnetically disordered, as described above. The decreased particle sizes of the quenched Ba_2FeReO_6 sample also demonstrate the trend toward smaller M_s value, though the % B/B′ ordering is fairly similar. For the flux-prepared Sr_2CrReO_6 products, spontaneous magnetizations of ~0.74−0.80 μ_B were smaller than the 1.0 μ_B predicted from the Cr^{3+}/Re^{5+} antiparallel alignment of spins. The M_s and M_r values primarily increased with an increasing % Cr/Re site ordering. In general, the coercivities of the Sr_2CrReO_6 products were much higher than for either Sr_2FeReO_6 or Ba_2FeReO_6.

For these $A_2BB'O_6$ double-perovskites in their polycrystalline forms, a large magnetoresistance has previously been found that originates from the grain boundaries serving as an insulating barrier in which the tunneling probability of electrons depend on the orientation of their moments between the grains.[2,6] Current theories show that the size of the intergrain tunneling magnetoresistance (i.e., ITMR) is dependent upon both the percent spin polarization and the concentration of grain

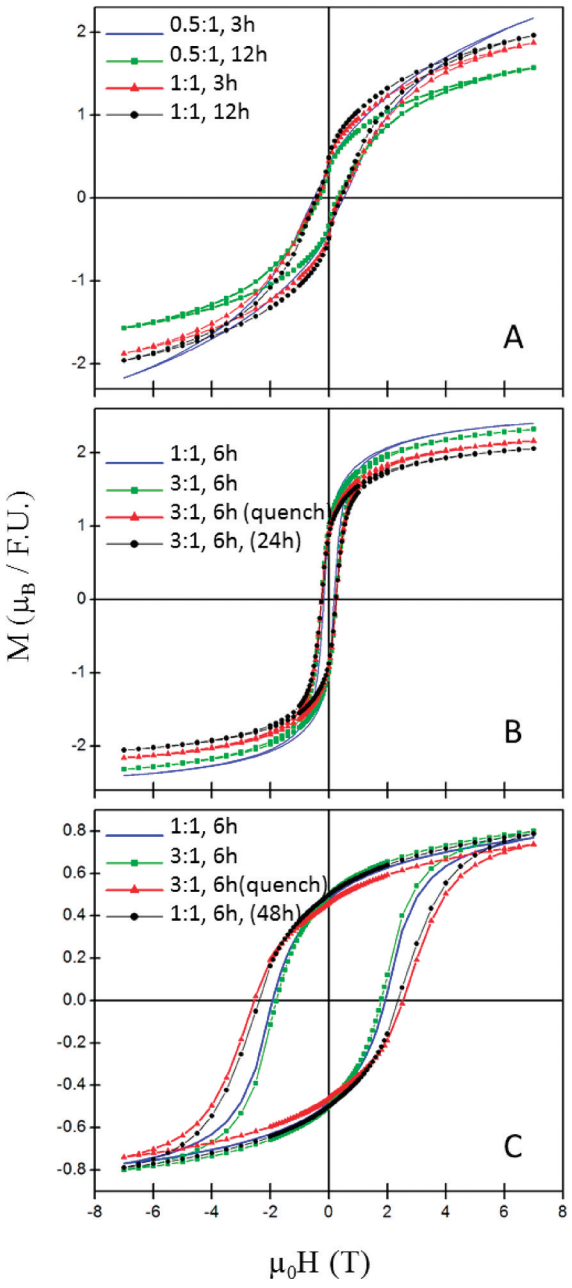

Figure 4. $M(H)$ curves for Sr_2FeReO_6 (A), Ba_2FeReO_6 (B), and Sr_2CrReO_6 (C) that were synthesized using a molten NaCl/KCl flux. Each curve is labeled according to the flux-to-product molar ratio (#:#), reaction time (#h), and cooling time (#h) if other than radiatively cooled.

boundaries. However, although the amount of spin polarization can reportedly be adjusted to near 100% with the appropriate combination of A/B/B′ cations,[3] the modulation of the grain boundaries through variations in particle sizes and surfaces has been restricted because of their conventional solid-state syntheses. Thus, the flux-prepared Sr_2FeReO_6, Ba_2FeReO_6, and Sr_2CrReO_6 particles were pressed into polycrystalline pellets without annealing and their temperature-dependent resistivities were measured. The resistivities of Sr_2FeReO_6 prepared by both solid-state and a 1:1 flux for 3 h, Ba_2FeReO_6 synthesized using a 1:1 flux and Sr_2FeReO_6 at a 1:1 flux (both radiatively cooled) are compared in Figure 5. All samples exhibit a semiconducting-type behavior consistent with previous reports. The flux prepared

Table 4. Magnetic Properties of the Flux-Prepared Double-Perovskites

	flux preparation (ratio, time)	M_s	H_c (T)	M_r (μ_B/F.U.)	B/B′ ordering (%)
Sr_2FeReO_6	0.5:1, 3 h	2.17	0.51	0.39	83
	0.5:1, 12 h	1.57	0.31	0.37	84
	1:1, 3 h	1.87	0.38	0.45	84
	1:1, 12 h	1.96	0.41	0.48	85
Ba_2FeReO_6	1:1, 6 h	2.40	0.18	0.98	90
	3:1, 6 h	2.32	0.25	0.98	94
	3:1, 6 h, (24 h)	2.10	0.25	0.87	97
	3:1, 6 h (quench)	2.16	0.25	0.92	90
Sr_2CrReO_6	1:1, 6 h	0.80	1.79	0.50	87
	3:1, 6 h	0.77	1.91	0.48	85
	3:1, 6 h (quench)	0.74	2.53	0.46	84
	1:1, 6 h, (48 h)	0.79	2.41	0.50	90

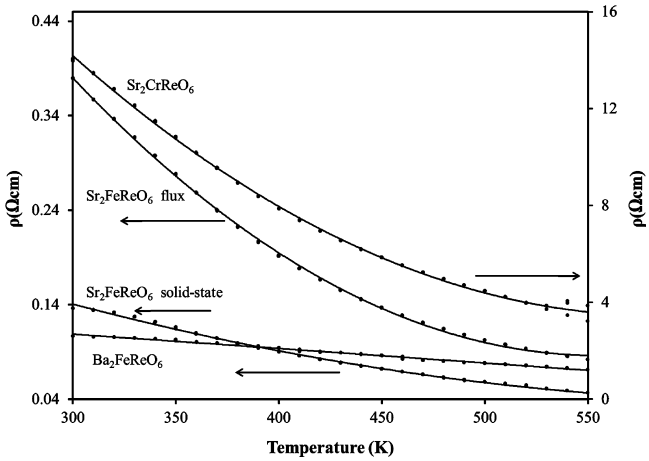

Figure 5. Temperature dependence of the resistivity for Sr_2FeReO_6 synthesized by the solid state method and at a 1:1 flux for 3 h; Ba_2FeReO_6 at a 1:1 flux for 6 h and radiatively cooled; and Sr_2CrReO_6 at a 1:1 flux for 6 h and radiatively cooled.

Sr_2FeReO_6 exhibited a greater temperature dependence and a resistivity about 3x higher than that of the solid-state sample, at ∼0.38−0.12 Ω cm (from 300−550 K) and ∼0.14−0.05 Ω cm, respectively. The resistivities of the flux-prepared Ba_2FeReO_6 and Sr_2CrReO_6 were a lower ∼0.07−0.1 Ω cm (300−550 K) and a higher ∼13−3 Ω cm, respectively. These measured resistivities are roughly 2−5× larger than the previously reported literature values,[2,4,27,28] which is likely the result of not sintering the pressed pellets as well as the increased concentration of grain boundaries. The latter is based on the fact that a higher resistance is associated with a higher concentration of insulating grain boundaries, but which also enhances the extent of the spin-dependent intergrain tunneling between particles.

Magnetoresistance measurements were taken with the application of a 3 kG magnetic field, with each exhibiting a remarkably large magnetoresistance that can be adjusted between ∼40−70% at room temperature depending on the particular double-perovskite and the flux-synthesis conditions. Shown in Figure 6, the magnetic-field dependence of the resistivity has been measured for both the solid-state and flux-prepared Sr_2FeReO_6 particles. The higher resistivity of the flux-prepared Sr_2FeReO_6 is accompanied by a slightly larger change in resistance with the magnetic field. This based on the fact that

dx.doi.org/10.1021/cm202545z | Chem. Mater. 2011, 23, 5409−5414

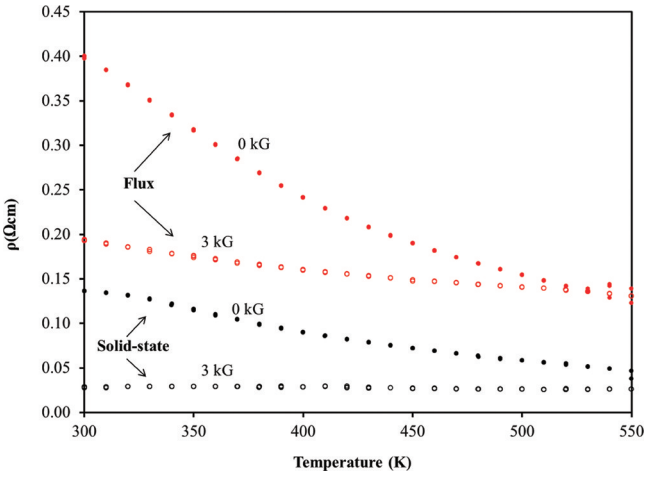

Figure 6. Temperature and magnetic-field dependence of the resistivity for polycrystalline Sr_2FeReO_6 pellets prepared via the solid-state and flux-synthetic routes (1:1 molar ratio, 3 h).

a higher resistance is associated with a higher concentration of insulating grain boundaries, but which also serves to likely enhance the extent of the spin-dependent intergrain tunneling between particles. Both Ba_2FeReO_6 and Sr_2CrReO_6 also appear to exhibit a similarly large ITMR at room temperature of up to ~65% and ~70% respectively, given in the Supporting Information. Such large polycrystalline magnetoresistances at low magnetic fields have only been previously reported for the more intensely studied Sr_2FeMoO_6 (ITMR of ~20–30% at 4 kG) when prepared as nanoscale particles of ~29–45 nm.[10]

CONCLUSIONS

The first flux-mediated syntheses have been investigated for three rhenium-containing members of the double-perovskite $A_2BB'O_6$ family, Sr_2FeReO_6, Ba_2FeReO_6, and Sr_2CrReO_6. Relatively rapid and efficient single-step reactions are demonstrated herein using a eutectic NaCl/KCl mixture that can be used to achieve a high purity and homogeneous distribution of particle sizes that are tunable between ~50 nm to >1 μm. Smaller particles could be obtained by decreasing the reaction times. Samples with smaller particle sizes have a greater concentration of grain boundaries and resulted in larger temperature dependent resistivities compared to solid-state samples. This new synthetic route enables deeper investigations of the effects of particle sizes and % B/B′ site ordering on their magnetic properties.

ASSOCIATED CONTENT

Supporting Information

Crystallographic data and PXRD Rietveld refinement results. This material is available free of charge via the Internet at http://pubs.acs.org/.

AUTHOR INFORMATION

Corresponding Author

*E-mail: paul_maggard@ncsu.edu.

ACKNOWLEDGMENTS

Financial support from the National Science Foundation (DMR-0644833) and access to a SQUID magnetometer (D. Shultz).

REFERENCES

(1) Kobayashi, K.-I.; Kimura, T.; Sawada, H.; Terakura, K.; Tokura, Y. *Nature* **1998**, *395*, 677–680.
(2) Kobayashi, K.-I.; Kimura, T.; Tomioka, Y.; Swada, H.; Terakura, K.; Tokura, Y. *Phys. Rev. B* **1999**, *59*, 159–162.
(3) Serrate, D.; De Teresa, J. M.; Ibarra, M. R. *J. Phys.: Condens. Matter* **2007**, *19*, 023201.
(4) Kato, H.; Okuda, T.; Okimoto, Y.; Tomioka, Y.; Oikawa, K.; Kamiyama, T.; Tokura, Y. *Phys. Rev. B* **2004**, *69*, 184412-1–184412-8.
(5) Kato, H.; Okuda, T.; Okimoto, Y.; Tomioka, Y.; Takenoya, Y.; Ohkubo, A.; Kawasaki, M.; Tokura, Y. *Appl. Phys. Lett.* **2002**, *81*, 328–330.
(6) Tomioka, Y.; Okuda, T.; Okimoto, Y.; Kumai, R.; Kobayashi, K.-I. *Phys. Rev. B* **2000**, *61*, 422–427.
(7) Hwang, H. Y.; Cheong, S. W.; Ong, N. P.; Batlogg. *Phys. Rev. Lett.* **1996**, *77*, 2041–2044.
(8) Balcells, J.; Navarro, M.; Bibes, M.; Roig, A.; Martinez, B.; Fontcuberta, J., *Appl. Phys. Lett.* **2001**, *78*, 781–783.
(9) Jacobo, S. E.; Duhalde, S.; Mercader, R. C. *Physica B* **2004**, *354*, 59–62.
(10) Yuan, C. L.; Wang, S. G.; Song, W. H.; Yu, T.; Dai, J. M.; Ye, S. L.; Sun, Y. P. *Appl. Phys. Lett.* **1999**, *75*, 3853–3855.
(11) Li, X. H.; Sun, Y. P.; Lu, W. J.; Ang, R.; Zhang, S. B.; Zhu, X. B.; Song, W. H.; Dai, J. M. *Solid State Commun.* **2008**, *145*, 98–102.
(12) Zhong, W.; Liu, W.; Au, C. T.; Du, Y. W. *Nanotechnology* **2006**, *17*, 250–256.
(13) Porob, D.; Maggard, P. A. *Mater. Res. Bull.* **2006**, *41*, 1513–1519.
(14) Porob, D.; Maggard, P. A. *J. Solid State Chem.* **2006**, *179*, 1727–1732.
(15) Arney, D.; Porter, B.; Greve, B.; Maggard, P. *J. Photochem. Photobiol. A: Chemistry* **2008**, *199*, 230–235.
(16) Arney, D.; Watkins, T.; Maggard, P. A. *J. Am. Ceram. Soc.* **2011**, *94*, 1483–1489.
(17) Prellier, W.; Smolyaninova, V.; Biswas, A.; Galley, C.; Greene, R. L.; Ramesha, K.; Gopalakrishnan, J. *J. Phys.: Condens. Matter* **2000**, *12*, 965–973.
(18) *Jade 9*; Materials Data Incorporated: Livermore, CA, 2009.
(19) Gopalakrishnan, J.; Chattopadhyay, A.; Ogale, S. B.; Venkatesan, T.; Greene, R. L.; Millis, A. J.; Ramesha, K.; Hannoyer, B.; Marest, G. *Phys. Rev. B* **2000**, *62*, 9538–9542.
(20) Retuerto, M.; Martinez-Lope, M. J.; Garcia-Hernandez, M.; Alonso, J. A. *Mater. Res. Bull.* **2009**, *44*, 1261–1264.
(21) Michalik, J. M.; De Teresa, J. M.Ritter, C.; Blasco, J.; Serrate, M. R.; Ibarra, M. R.; Kapusta, C.; Freundenberger, J.; Kozlova, N. *Europhys. Lett.* **2007**, *78*, 17006-p1–17006-p6.
(22) De Teresa, J. M.; Michaelik, J. M.Blasco, J.; Algarabel, P. A.; Ibarra, M. R., *Appl. Phys. Lett.* **2007**, *90*, 252514-1–252514-3.
(23) Michalik, J. M.; De Teresa, J. M.; Blasco, J.; Algarabel, P. A.; Ibarra, M. R.; Kapusta, Cz.; Zeitler, U. *J. Phys.: Condens. Matter* **2007**, *19*, 1–11.
(24) Lin, C.; Chu, Y.; Wang, S. *Mater. Lett.* **2006**, *60*, 2270–2273.
(25) Greneche, J. M.; Venkatesan, M.; Suryanarayanan, R.; Coey, J. M. D. *Phys. Rev. B* **2001**, *63*, 174403-1–174403-5.
(26) Yin, H. Q.; Zhou, J.-S.; Dass, R.; Zhou, J.-P.; McDevitt, J. T.; Goodenough, J. B. *J. Appl. Phys.* **2000**, *87*, 6761–6763.
(27) Alamelu, M.; Varadaraju, U. V.; Venkatesan, M.; Douvalis, A. P.; Coey, J. M. D. *J. Appl. Phys.* **2002**, *91*, 8909–8911.
(28) Teresa, J. M.; Serrate, D.; Blasco, J.; Ibarra, M. R.; Morellon, L. *Phys. Rev. B* **2004**, *69*, 14401-1–14401-10.